J Mater Sci (2009) 44:5383–5392
DOI 10.1007/s10853-009-3647-9

FERROELECTRICS

Ferroelastic interactions in bilayered ferroelectric thin films

R. Mahjoub · V. Anbusathaiah · V. Nagarajan

Received: 7 May 2009 / Accepted: 27 May 2009 / Published online: 19 June 2009

Abstract We present a theoretical investigation of the elastic interactions in a heteroepitaxial bilayer consisting of a (001) tetragonal $PbZr_xTi_{1-x}O_3$ and (001) rhombohedral $PbZr_{1-x}Ti_xO_3$ on a thick (001) passive substrate. Analytical expressions for the elastic interaction energies between the layers and the resultant ferroelastic twin formation have been derived as a function of the lattice misfit strain (between layers and the substrate), composition of the ferroelectric and thickness. It is found that the elastic coupling between the tetragonal and rhombohedral layers leads to the equilibrium domain fraction in the tetragonal layer several time larger than that in single-layer films of similar thickness. Most critically, the model finds a significant change in the ferroelastic domain volume fraction in the presence of an applied electric field and hence enhanced piezoelectric properties compared to single-layered epitaxial PZT thin films.

Introduction

Recently, there has been significant interest in multilayered ferroelectric thin films as they have been demonstrated to show enhanced functional properties such as polarization [1–4], and dielectric permittivity [5–7]. It has also been found that the close proximity of ferroelectric layers with varying compositions can also lead to new structural phases [3]. These observations have been explained on the basis of electric field-induced coupling [8], epitaxial strain [6, 9, 10], and specific polar interactions between the interfacial layers [2, 11]. One interesting aspect in the case of ferroelectric thin films is that the transformation from paraelectric (PE-high symmetry) state to the ferroelectric state (FE-low symmetry) leads to a remnant self-strain and hence the PE → FE phase transition has an elastic energy component associated with it. In order to relax this excess elastic energy, ferroelastic domains are formed in the film [12, 13]. Indeed, ferroelastic domain evolution [14, 15], morphology [16, 17], and behavior under electric field [18] have significant contribution to the ultimate physical properties of the thin film. The magnitude of this self-strain is of course compositionally dependent; however, typically in tetragonal ferroelectrics with large spontaneous polarization (such as $PbTiO_3$) it is very high (∼of the order of 5%) in the bulk material alone. Thus one may consider that in the case of multilayers that have compositions of a strongly tetragonal FE, one requires an elastic coupling between the layers based upon the concept of equal and opposite tractions [19] in order to maintain a mechanically stable interface between the FE layers. The implications of such an elastic coupling in addition to the two-dimensional constraints imposed by the substrate must affect the total free energy of the structure and may yield physical properties which cannot be observed in corresponding epitaxial single-layer thin films.

Recently, we showed that an elastic coupling arising from equal and oppositely signed tractions between the two functional layers (i.e., in an epitaxial bilayer consisting of a tetragonal (T) $PbZr_xTi_{1-x}O_3$ (PZT) film, and a rhombohedral (R) PZT film on a thick cubic substrate) may yield indirect elastic interactions between them resulting in an enhanced volume fraction of the domains with in-plane polarization (referred to as *a*-domains or polydomains

R. Mahjoub · V. Anbusathaiah · V. Nagarajan (✉)
School of Materials Science and Engineering, University of New South Wales, Sydney, NSW 2052, Australia
e-mail: nagarajan@unsw.edu.au

here) [20]. In this paper, we provide a detailed numerical analysis of how these elastic interaction energies come into play due to such traction effects in [001]-oriented epitaxial PZT bilayer thin films. Tensorial analysis is coupled with linear elasticity theory [21] to compute the contributions of the microstrain energies between the ferroelastic domain walls, the layer thickness, misfit strain as well as composition on the polydomain fraction. Furthermore, it is shown that the ferroelastic polydomain structure in the T layer is highly susceptible to external electric field as it is no longer constrained by the bottom thick cubic substrate. Consequently, giant piezoelectric coefficients (particularly d_{33}) are anticipated.

Theory

As mentioned previously, the theory developed is for [001]-oriented epitaxial PZT bilayer thin films. The deposition history of the films is properly addressed by taking into account the effective misfit strain between the film at cubic phase and the effective substrate lattice parameter [13] at growth temperature. The effect of thickness is transmitted as a strain relaxation process caused by the formation of (misfit) dislocations at the interfaces between layers [22]. As illustrated in the schematic (Fig. 1), h_T and h_R are the thicknesses of the top tetragonal (T) and bottom rhombohedral (R) layers, respectively. A is the interface area and D is the domain periodicity of the twin domains, which have been assumed to be much smaller than the film thicknesses. Consequently, the dense domain model can be applied and strain fields are considered homogeneous within the domains. The free energy of the individual thin film is calculated as the product of its free energy density and the volume, and the total free energy, F_{total} of the bilayered thin film structure is the sum of the free energies of each layer and it is expressed as

$$F_{total} = F_T \times h_T \times A + F_R \times h_R \times A \tag{1}$$

where F_T and F_R are the free energy densities of T and R layers, which are given by

$$F_T = F_{T-el} + \alpha F_{a-0} + (1-\alpha)F_{c-0} \quad \text{and}$$
$$F_R = F_{R-el} + F_{R-0} \tag{2}$$

In Eq. 2, α and $1-\alpha$ are the volume fractions of a and c domains in the tetragonal layer, F_{a-0}, F_{c-0}, and F_{R-0} are the free energy densities of the undistorted domains, $F_{T-el} = \hat{\varepsilon}_T\hat{\sigma}_T/2$ and $F_{R-el} = \hat{\varepsilon}_R\hat{\sigma}_R/2$ are the elastic energy density of T and R films, respectively.

The macroscopic strains and stresses in c and a domains and R layer can be approximated as the average strains and stresses, created by the average mismatch between the domains and neighboring layers [12]. Therefore in the T layer, the total strain tensor $\hat{\varepsilon}_T$ can be expressed as the average of the elastic strain tensors of its domains, weighted by their corresponding volume fractions:

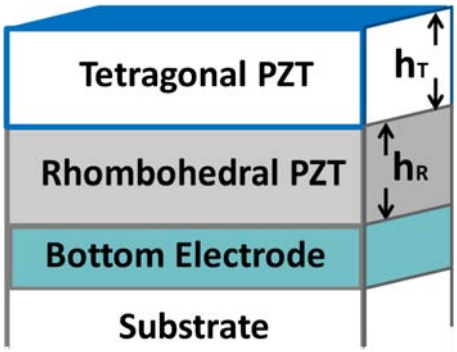

Fig. 1 Schematic of the bilayer

$$\hat{\varepsilon}_T = \alpha\hat{\varepsilon}_{T,a} + (1-\alpha)\hat{\varepsilon}_{T,c} \tag{3}$$

where $\hat{\varepsilon}_{T,a}$ and $\hat{\varepsilon}_{T,c}$ are the strain tensors in the a and c domains, respectively. We begin our analysis under zero electric field. In each domain or phase, the total strain is equal to the summation of the self-strain tensor and misfit strain tensor:

$$\hat{\varepsilon}_{T,c} = \hat{\varepsilon}^0_{T,c} + \hat{u}_{M,T},\ \hat{\varepsilon}_{T,a} = \hat{\varepsilon}^0_{T,a} + \hat{u}^0_{M,T} \quad \text{and}$$
$$\hat{\varepsilon}_R = \hat{\varepsilon}^0_R + \hat{u}^0_{M,R} \tag{4}$$

The self-strain tensors of the domains in the tetragonal and the rhombohedral layers are defined as

$$\hat{\varepsilon}^0_{T,c} = \begin{bmatrix} \varepsilon_1 & 0 & 0 \\ 0 & \varepsilon_1 & 0 \\ 0 & 0 & \varepsilon_3 \end{bmatrix},\ \hat{\varepsilon}^0_{T,a} = \begin{bmatrix} \varepsilon_3 & 0 & 0 \\ 0 & \varepsilon_1 & 0 \\ 0 & 0 & \varepsilon_1 \end{bmatrix},$$
$$\hat{\varepsilon}^0_R = \begin{bmatrix} \varepsilon_R & \gamma & \gamma \\ \gamma & \varepsilon_R & \gamma \\ \gamma & \gamma & \varepsilon_R \end{bmatrix} \tag{5}$$

where γ is the shear strain [23]. These self-strains are introduced in the thin film structure during their phase transition from the paraelectric phase into the subsequent tetragonal or rhombohedral phase at Curie temperature, T_c. The strain components induced in this process can be expressed as

$$\varepsilon_1 = (a_{cubic,T} - a_T)/a_{cubic,T},$$
$$\varepsilon_3 = (a_{cubic,T} - c_T)/a_{cubic,T} \text{ and}$$
$$\varepsilon_R = (a_{cubic,R} - a_R)/a_{cubic,R} \tag{6}$$

At higher growth and annealing temperatures, the Ti-rich and the Zr-rich PZT layers are both in paraelectric phase, having the lattice parameters equal to $a_{cubic,T}$ and $a_{cubic,T}$, respectively, thereby giving rise to a misfit strain, $u_{m,R}$ at T_c between the sandwiched thin films and the thick substrate as follows:

$$u_{\mathrm{m,R}} = \frac{\left(a_{\mathrm{S}}^{*} - a_{\mathrm{cubic,R}}\right)}{a_{\mathrm{S}}^{*}} \tag{7}$$

Similarly, the misfit strain, $u_{\mathrm{m,T}}$ between the two thin film layers can be written as:

$$u_{\mathrm{m,T}} = \frac{\left(a_{\mathrm{cubic,R}}^{*} - a_{\mathrm{cubic,T}}\right)}{a_{\mathrm{cubic,R}}^{*}} \tag{8}$$

where a_{S}^{*} and $a_{\mathrm{cubic,R}}^{*}$ are the effective lattice parameters of the substrate and R film for which the effect of dislocation relaxation has been included. These effective lattice parameters can be expressed as

$$a_{\mathrm{S}}^{*}(h, T_{\mathrm{G}}) = \frac{a_{\mathrm{S}}(T_{\mathrm{G}})}{\rho_{\mathrm{S}}(h, T_{\mathrm{G}}) \times a_{\mathrm{S}}(T_{\mathrm{G}}) + 1} \quad \text{and}$$
$$a_{\mathrm{cubic,R}}^{*}(h, T_{G}) = \frac{a_{\mathrm{cubic,R}}(T_{\mathrm{G}})}{\rho_{\mathrm{R}}(h, T_{\mathrm{G}}) \times a_{\mathrm{cubic,R}}(T_{\mathrm{G}}) + 1} \tag{9}$$

where ρ is the linear dislocation density and T_{G} is the deposition temperature.

A cubic thick substrate will induce axial in-plane misfit strains into the film and the out of plane strain can be calculated in terms of these in-plane components. Moreover, the mechanical boundary conditions of a thin film (i.e., plane-stress) require that the out of plane stresses of the film vanish. Finally, due to the *m3m* symmetry of the anisotropic cubic structure of the PZT at growth temperature only three components of the film elastic moduli matrix can be nonzero and independent. Therefore from Hooke's law, the out of plane strain components are obtained as:

$$\sigma_{11} = C_{11}u_{\mathrm{m}} + C_{12}u_{\mathrm{m}} + C_{12}\varepsilon_{33} \tag{10}$$
$$\sigma_{22} = C_{12}u_{\mathrm{m}} + C_{11}u_{\mathrm{m}} + C_{12}\varepsilon_{33} \tag{11}$$
$$\sigma_{33} = C_{12}u_{\mathrm{m}} + C_{12}u_{\mathrm{m}} + C_{11}\varepsilon_{33} = 0 \tag{12}$$
$$\sigma_{23} = 2C_{44}\varepsilon_{23} = 0 \tag{13}$$
$$\sigma_{31} = 2C_{44}\varepsilon_{31} = 0 \tag{14}$$
$$\sigma_{12} = 2C_{44}\varepsilon_{12} \tag{15}$$

Hence the misfit tensors of the T and R layers can be expressed as

$$\hat{u}_{\mathrm{M,T}} = \begin{pmatrix} u_{\mathrm{m,T}} & 0 & 0 \\ 0 & u_{\mathrm{m,T}} & 0 \\ 0 & 0 & (-2C_{12}/C_{11})u_{\mathrm{m,T}} \end{pmatrix},$$
$$\hat{u}_{\mathrm{M,R}} = \begin{pmatrix} u_{\mathrm{m,R}} & 0 & 0 \\ 0 & u_{\mathrm{m,R}} & 0 \\ 0 & 0 & (-2C_{12}/C_{11})u_{\mathrm{m,R}} \end{pmatrix} \tag{16}$$

Using the effective lattice parameter allows us to incorporate the effect of film thicknesses into the final strain tensors. In case of silicon substrates, where the interfacial strain is dominated by thermal mismatch, approximate evaluation of the thermally induced strains in single and bilayered heterostructures are made according to which $u_{\mathrm{m,R}} = \Delta\lambda \cdot \Delta T$ [24] where $\Delta\lambda = \lambda_{\mathrm{PZT}} - \lambda_{\mathrm{Si}}$ and λ is the coefficient of thermal expansion.

The mechanical equilibrium condition between the T and R layers requires that the tractions at the interface between these layers be equal and opposite at both sides, i.e., $f_{\mathrm{R},||} = -f_{\mathrm{T},||}$ [25]. This condition can also be regarded as the elastic coupling between the two films. Thus, $\sigma_{\mathrm{R},||} \times h_{\mathrm{R}} = -\sigma_{\mathrm{T},||} \times h_{\mathrm{T}}$ and can be expanded in terms the *planar elastic moduli* $\hat{\hat{G}}$ as $\hat{\hat{G}}_{\mathrm{R}}\hat{\varepsilon}_{\mathrm{R}}h_{\mathrm{R}} = -\hat{\hat{G}}_{\mathrm{T}}\hat{\varepsilon}_{\mathrm{T}}h_{\mathrm{T}}$ where $\hat{\hat{G}}$ is a fourth-rank tensor and is dependent on the bulk elastic moduli $\hat{\hat{C}}$, as well as the normal vector to the interface plane **n** and is expressed in tensor notation as [26]

$$\hat{\hat{G}} = \hat{\hat{C}} - \hat{\hat{C}}\vec{n}\left(\vec{n}\hat{\hat{C}}\vec{n}\right)^{-1}\vec{n}\hat{\hat{C}} \tag{17}$$

The total stress in the T layer can be considered as linearly proportional to the average macrostrains induced in this layer namely,

$$\hat{\sigma}_{\mathrm{T}} = \hat{\hat{G}}_{\mathrm{T}}(\alpha\hat{\varepsilon}_a + (1-\alpha)\hat{\varepsilon}_c) \tag{18}$$

Based on the above definitions and by applying the plane-stress mechanical boundary conditions between the two layers, the elastic energies of the heterostructure can be expanded as

$$F_{\mathrm{T-el}} = \frac{1}{2}(\alpha\hat{\varepsilon}_a + (1-\alpha)\hat{\varepsilon}_c)\hat{\hat{G}}_{\mathrm{T}}(\alpha\hat{\varepsilon}_a + (1-\alpha)\hat{\varepsilon}_c) \tag{19}$$
$$F_{\mathrm{R-el}} = \frac{1}{2}\hat{\varepsilon}_{\mathrm{R}}\left(\frac{-h_{\mathrm{T}}}{h_{\mathrm{R}}}\hat{\sigma}_{\mathrm{T}}\right) = \frac{1-h_{\mathrm{T}}}{2\ h_{\mathrm{R}}}\hat{\varepsilon}_{\mathrm{R}}\hat{\hat{G}}_{\mathrm{T}}(\alpha\hat{\varepsilon}_a + (1-\alpha)\hat{\varepsilon}_c) \tag{20}$$
$$F_{\mathrm{T-el}} = \frac{1}{2}\alpha^2\hat{\varepsilon}_a\hat{\hat{G}}_{\mathrm{T}}\hat{\varepsilon}_a + \frac{1}{2}(1-\alpha)^2\hat{\varepsilon}_c\hat{\hat{G}}_{\mathrm{T}}\hat{\varepsilon}_c + \alpha(1-\alpha)\hat{\varepsilon}_a\hat{\hat{G}}_{\mathrm{T}}\hat{\varepsilon}_c \tag{21}$$
$$F_{\mathrm{R-el}} = \frac{-h_{\mathrm{T}}}{2h_{\mathrm{R}}}\alpha\hat{\varepsilon}_{\mathrm{R}}\hat{\hat{G}}_{\mathrm{T}}\hat{\varepsilon}_a + \frac{-h_{\mathrm{T}}}{2h_{\mathrm{R}}}(1-\alpha)\hat{\varepsilon}_{\mathrm{R}}\hat{\hat{G}}_{\mathrm{T}}\hat{\varepsilon}_c \tag{22}$$

The elastic energies of the *c*- and *a*-domains are expressed as

$$e_{c,\mathrm{T}} = \frac{1}{2}\hat{\varepsilon}_c\hat{\hat{G}}_{\mathrm{T}}\hat{\varepsilon}_c \quad \text{and} \quad e_{a,\mathrm{T}} = \frac{1}{2}\hat{\varepsilon}_a\hat{\hat{G}}_{\mathrm{T}}\hat{\varepsilon}_a \tag{23}$$

The elastic interaction energy which is the part of the misfit energy that depends only on the difference between the domains or phases or in a ferroelastic thin film is given [12] as

$$e_{ca,\mathrm{T}}^{\mathrm{I}} = \frac{1}{2}(\hat{\varepsilon}_c - \hat{\varepsilon}_a)\hat{\hat{G}}_{\mathrm{T}}(\hat{\varepsilon}_c - \hat{\varepsilon}_a) \tag{24}$$

It is noted that if the planar elastic moduli is derived in terms of the normal direction to the interface of the film

and the substrate (**n**) then Eq. 24 yields indirect interaction energy, conversely if it is calculated in terms of the normal to the domain wall (**m**), it is called the direct interaction energy.

In the case of a bilayered film, the concept of indirect elastic interaction energy between two phases is farther expanded. We incorporate an indirect interaction energy between c-domain in the T layer and the underlying R layer. This is defined as

$$e^{\mathrm{I}}_{c\mathrm{R,T}} = \frac{1}{2}(\hat{\varepsilon}_c - \hat{\varepsilon}_\mathrm{R})\hat{\hat{G}}_\mathrm{T}(\hat{\varepsilon}_c - \hat{\varepsilon}_\mathrm{R}) \tag{25}$$

Similarly, by definition the indirect interaction energy between a-domain and the sandwiched R layer may be expressed as

$$e^{\mathrm{I}}_{a\mathrm{R,T}} = \frac{1}{2}(\hat{\varepsilon}_a - \hat{\varepsilon}_\mathrm{R})\hat{\hat{G}}_\mathrm{T}(\hat{\varepsilon}_a - \hat{\varepsilon}_\mathrm{R}) \tag{26}$$

A simple mathematical rearrangement will yield

$$e^{\mathrm{I}}_{a\mathrm{R,T}} = e_{a,\mathrm{T}} + e_{\mathrm{R,T}} - \hat{\varepsilon}_a\hat{\hat{G}}_\mathrm{T}\hat{\varepsilon}_\mathrm{R} \tag{27}$$

$$e^{\mathrm{I}}_{c\mathrm{R,T}} = e_{c,\mathrm{T}} + e_{\mathrm{R,T}} - \hat{\varepsilon}_c\hat{\hat{G}}_\mathrm{T}\hat{\varepsilon}_\mathrm{R} \tag{28}$$

Next the elastic energies of the structure are expressed in terms of the aforementioned interaction energies:

$$F_{\mathrm{T-el}} = \alpha^2 e_{a,\mathrm{T}} + (1-\alpha)^2 e_{c,\mathrm{T}} + \alpha(1-\alpha)\left(e_{a,\mathrm{T}} + e_{c,\mathrm{T}} - e^{\mathrm{I}}_{ac,\mathrm{T}}\right) \tag{29}$$

$$F_{\mathrm{R-el}} = -\frac{h_\mathrm{T}}{2h_\mathrm{R}}\left[\alpha\left(e_{a,\mathrm{T}} + \frac{1}{2}\hat{\varepsilon}_\mathrm{R}\hat{\hat{G}}_\mathrm{T}\hat{\varepsilon}_\mathrm{R} - e^{\mathrm{I}}_{a\mathrm{R,T}}\right) + (1-\alpha)\left(e_{c,\mathrm{T}} - e^{\mathrm{I}}_{c\mathrm{R,T}}\right)\right] \tag{30}$$

$$F_{\mathrm{T-el}} = \alpha^2 e^{\mathrm{I}}_{ac,\mathrm{T}} + \alpha\left(e_{a,\mathrm{T}} - e_{c,\mathrm{T}} - e^{\mathrm{I}}_{ac,\mathrm{T}}\right) + e_{c,\mathrm{T}} \tag{31}$$

$$F_{\mathrm{R-el}} = -\frac{h_\mathrm{T}}{2h_\mathrm{R}}\left[\alpha\left(e_{a,\mathrm{T}} - e_{c,\mathrm{T}} - e^{\mathrm{I}}_{a\mathrm{R,T}} + e^{\mathrm{I}}_{c\mathrm{R,T}}\right) + \left(\frac{1}{2}\hat{\varepsilon}_\mathrm{R}\hat{\hat{G}}_\mathrm{T}\hat{\varepsilon}_\mathrm{R} + e_{c,\mathrm{T}} - e^{\mathrm{I}}_{c\mathrm{R,T}}\right)\right] \tag{32}$$

Finally, the total free energy of the structure is written as

$$F_{\mathrm{total}} = Ah_\mathrm{T}\left[\alpha^2 e^{\mathrm{I}}_{ac,\mathrm{T}} + \alpha\left(e_{a,\mathrm{T}} - e_{c,\mathrm{T}} - e^{\mathrm{I}}_{ac,\mathrm{T}}\right) + e_{c,\mathrm{T}}\right] + Ah_\mathrm{R}\left[-\frac{h_\mathrm{T}}{2h_\mathrm{R}}\left[\alpha\left(e_{a,\mathrm{T}} - e_{c,\mathrm{T}} - e^{\mathrm{I}}_{a\mathrm{R,T}} + e^{\mathrm{I}}_{c\mathrm{R,T}}\right) + \left(\frac{1}{2}\hat{\varepsilon}_\mathrm{R}\hat{\hat{G}}_\mathrm{T}\hat{\varepsilon}_\mathrm{R} + e_{c,\mathrm{T}} - e^{\mathrm{I}}_{c\mathrm{R,T}}\right)\right]\right] + Ah_\mathrm{T}F_{\mathrm{T}-0} + Ah_\mathrm{R}F_{\mathrm{R}-0} \tag{33}$$

It should be pointed out that the direct interaction energy between two domains depends on the normal vector to the interface between them (**m**) rather than their common interface with the substrate. However, it can be shown that the direct interaction energy between these two domains or phases are several orders of magnitude smaller than the indirect interaction energy between them in either single or bilayerd structures and can hence be neglected in the calculation of the structure total energy [27].

At equilibrium the a-domain volume fraction is so chosen that the multilayer free energy becomes minimal. By setting $\partial F_{\mathrm{total}}/\partial\alpha$ to zero, the equilibrium value for α is obtained as

$$\alpha_{\mathrm{bilayer}} = \frac{(e_{c,\mathrm{T}} - e_{a,\mathrm{T}} + 2e^{\mathrm{I}}_{ca,\mathrm{T}} + e^{\mathrm{I}}_{c\mathrm{R,T}} - e^{\mathrm{I}}_{a\mathrm{R,T}})}{4e^{\mathrm{I}}_{ca,\mathrm{T}}} + \frac{\Delta F_0}{2e^{\mathrm{I}}_{ca,\mathrm{T}}} \tag{34}$$

where $\Delta F_0 = (F_{c-0} - F_{a-0})$ and connotes the difference between free energy densities of the undistorted structures in the T layer. On the other hand, it can easily be illustrated that in a simple structure comprising a tetragonal PZT and a passive substrate, the equilibrium 'a' domain volume fraction is

$$\alpha_{\mathrm{Tlayer-substrate}} = \frac{(e_{c,\mathrm{T}} - e_{a,\mathrm{T}} + e^{\mathrm{I}}_{ca,\mathrm{T}})}{2e^{\mathrm{I}}_{ca,\mathrm{T}}} + \frac{\Delta F_0}{2e^{\mathrm{I}}_{\mathrm{ca,T}}} \tag{35}$$

Equation (33) can be minimized only if $e^{\mathrm{I}}_{\mathrm{ca,T}} > 0$. Moreover, by definition this condition should always be satisfied: $1 - \Delta F_0/2e^{\mathrm{I}}_{ca,\mathrm{T}} \geq \Delta\alpha \geq -\Delta F_0/2e^{\mathrm{I}}_{ca,\mathrm{T}}$.

It should be noted that in the right-hand side of the Eqs. 34 and 35, ΔF_0 and the interaction energy of a and c-domains, i.e., $e^{\mathrm{I}}_{ca,\mathrm{T}}$, are constant and do not depend on strains. As a result, the change of the equilibrium a-domain volume fraction in both structures can be expressed as

$$\Delta\alpha_{\mathrm{bilayer}} = \frac{(e_{c,\mathrm{T}} - e_{a,\mathrm{T}} + 2e^{\mathrm{I}}_{ca,\mathrm{T}} + e^{\mathrm{I}}_{c\mathrm{R,T}} - e^{\mathrm{I}}_{a\mathrm{R,T}})}{4e^{\mathrm{I}}_{ca,\mathrm{T}}} \quad \text{and}$$

$$\Delta\alpha_{\mathrm{single-layer}} = \frac{(e_{c,\mathrm{T}} - e_{a,\mathrm{T}} + e^{\mathrm{I}}_{ca,\mathrm{T}})}{2e^{\mathrm{I}}_{ca,\mathrm{T}}} \tag{36}$$

Additionally, if F is considered to be the Helmholtz free energy, then F_c and F_a are equal and the last terms on the right-hand side of Eqs. 34 and 35 vanish. As a result, the equilibrium a-domain volume fraction in both structures can be expressed as

$$\alpha_{\mathrm{bilayer}} = \frac{(e_{c,\mathrm{T}} - e_{a,\mathrm{T}} + 2e^{\mathrm{I}}_{ca,\mathrm{T}} + e^{\mathrm{I}}_{c\mathrm{R,T}} - e^{\mathrm{I}}_{a\mathrm{R,T}})}{4e^{\mathrm{I}}_{ca,\mathrm{T}}} \text{ and}$$

$$\alpha_{\mathrm{single-layer}} = \frac{(e_{c,\mathrm{T}} - e_{a,\mathrm{T}} + e^{\mathrm{I}}_{ca,\mathrm{T}})}{2e^{\mathrm{I}}_{ca,\mathrm{T}}} \tag{37}$$

It follows from equation (37) that the elastic energies and specifically those energies created by the interaction strains between the ferroelastic domains and the rhombohedral structure defined in Eqs. 25 and 26, significantly affect the

ferroelastic domain volume fraction. These interactions and their respective energies are controlled by effective misfits induced in the structure. Moreover, different signs of these elastic interaction energies (positive for the interaction of the *c*-domain with R and negative for that of *a*-domain) behave as a negative feedback loop which controls the ferroelastic domains of the structure so that an increase in the interaction energy of *c*-domain will boost the *a*-domain fraction and vice versa.

Additionally, the contribution of the walls between the microstructures in the T layer to the total free energy can be taken into account. This will yield the incompatibility parameter which is the ratio of the energies of direct and direct interactions between the domains and can be expressed as $\eta_N = \eta'/\sqrt{h}$ where $\eta' = \sqrt{h_{cr}}/(1-\beta)$ is the effective incompatibility, h_{cr} is the critical thickness of domain formation and β is the ratio of the T layer thickness to the total film thickness [21]. Consequently, the equilibrium *a*-domain fraction will be expressed as

$$\alpha^0 = \frac{e_{c,T} - e_{a,T} + 2(1-\eta_N)e^I_{ca,T} + e^I_{cR,T} - e^I_{aR,T}}{4(1-\eta_N)e^I_{ca,T}} \tag{38}$$

The effect of external electric field on the ferroelastic domain formation can be predicted by incorporating the linear piezoelectric strain caused by the field into the strain tensor. The constraints imposed by the thick substrate on R layer will modify its effective out-of-plane piezoelectric coefficient as [6]

$$d_{33-\text{film}} = d_{33-\text{bulk}} - 2\frac{S_{13}}{S_{11}+S_{12}}d_{31-\text{bulk}} \tag{39}$$

The effective d_{31} and d_{32} of the R layer will vanish to zero (as it is clamped) and its electrostrictive coefficient will be changed to $Q_{\text{eff}} = Q_{11} + \xi_P Q_{12}$ where $\xi_P = -2S^P_{13}/(S^P_{11} + S^P_{12})$ [28]. The piezoelectric and electrostrictive coefficients of the T layer remain the same as bulk. Thus the strain tensors in Eq. 5 are expressed as

$$\hat{\varepsilon}^0_{T,c} = \begin{bmatrix} \varepsilon_1 + d_{31,T}E_{3,T} & 0 & 0 \\ 0 & \varepsilon_1 + d_{32,T}E_{3,T} & 0 \\ 0 & 0 & \varepsilon_3 + d_{33,T}E_{3,T} \end{bmatrix} \tag{40}$$

$$\hat{\varepsilon}^0_{T,a} = \begin{bmatrix} \varepsilon_3 + d_{31,T}E_{3,T} & 0 & 0 \\ 0 & \varepsilon_1 + d_{32,T}E_{3,T} & 0 \\ 0 & 0 & \varepsilon_1 + d_{33,T}E_{3,T} \end{bmatrix} \tag{41}$$

$$\hat{\varepsilon}^0_{R} = \begin{bmatrix} \varepsilon_R & \gamma & \gamma \\ \gamma & \varepsilon_R & \gamma \\ \gamma & \gamma & \varepsilon_R + d_{33,R}E_{3,R} \end{bmatrix} \tag{42}$$

where

$$E_{3,T} = (h_T + h_R)E_3 \Big/ \left(h_T + \left(\frac{\chi_T + 1}{\chi_R + 1}\right)h_R\right) \quad \text{and}$$

$$E_{3,R} = (h_T + h_R)E_3 \Big/ \left(h_R + \left(\frac{\chi_R + 1}{\chi_T + 1}\right)h_T\right).$$

Moreover, the effective out-of-plane piezoelectric coefficient of the bilayer structure can be approximated by $\langle S_3 \rangle / E_3$ where

$$\langle S_3 \rangle = \alpha S_{3,a} + (1-\alpha)S_{3,c} + S_{3,R} \tag{43}$$

is the average of the out-of-plane strains in the *a*-domain, *c*-domain, and R layer, respectively, and are expressed as

$$S_{3,a} = \frac{(um1 + Q_{12,T}(P_{s,T} + \chi_{31,T}E_{3,a})^2)}{2} \tag{44}$$

$$S_{3,c} = \frac{(um1 + Q_{11,T}(P_{s,T} + \chi_{33,T}E_{3,c})^2)}{2} \tag{45}$$

$$S_{3,R} = \frac{(um2 + (2Q_{12,R} + Q_{12,R})(P_{s,R} + \chi_{33,R}E_{3,R})^2)}{2} \tag{46}$$

where

$$\chi_{ij,T},\ \chi_{ij,R},\ P_{s,T} = \sqrt{|\varepsilon_3 Q_{11,T}|} \quad \text{and}$$

$$P_{s,R} = \sqrt{|\varepsilon_R(2Q_{12,R} + Q_{11,R})|}$$

are the electric susceptibilities and spontaneous polarizations of the T and R layers, respectively. It should be pointed out that χ_{31} is zero [29].

We note that this analysis does not take into account Clausius-Clapeyron type of effects on the polarization in the R and T layers due to the respective internal stress states in both layers [6, 30]. Furthermore, in these calculations neither long-scale electrostatics nor short-range dipole–dipole interactions between the layers were considered. Our approach presents a methodology based on mechanical equilibrium in the continuum limit. While these contributions might give rise to the formation of unique electrical domain structures within the R layer and the *c*/*a*/*c*/*a* polydomain structure, the mechanical domains in the T layer is expected to remain unchanged since there are no variations in the mechanical boundary conditions. Indeed, experimental results show that for 400 nm thick epitaxial tetragonal (001) $PbZr_{0.2}Ti_{0.8}O_3$ layer on (001) STO substrates with a dense *c*/*a*/*c*/*a* domain structure, there is no change in the stress state in the film and the domain fraction does not vary regardless of the electrical boundary conditions [31]. As such, ferroelectric polytwin structures may be thought of as purely ferroelastic domains.

Results and discussions

For the theory developed above, we examine two specific compositions in the PZT bilayered structure namely, PbZr20Ti80O3/$PbZr_{80}Ti_{20}O_3$/substrate or PZT (20/80) system and $PbZr_{40}Ti_{60}O_3$/$PbZr_{60}Ti_{40}O_3$/substrate or PZT (40/60) system. These two systems were chosen such as to understand the role of tetragonality in determining the equilibrium domain fractions in the T layer. $PbZr_{0.2}Ti_{0.8}O_3$ is of a higher tetragonality than that of $PbZr_{0.4}Ti_{0.6}O_3$ and the comparison of the results obtained for these two systems will illustrate the effect of tetragonality on physical properties of the bilayered structure.

It is evident that the ferroelastic domain fraction as calculated in Eq. 37 depends on elastic and elastic interaction energies. In the bilayered structure, two new terms pertaining to the elastic interactions between the two layers appear in the numerator. Figure 2a and b shows the elastic interaction energies between *c* domain—R layer ($e^{I}_{cR,t}$) and *a* domain—R layer ($e^{I}_{aR,T}$) as functions of T and R layer misfits in the PZT (20/80) system, respectively. It can be seen that a tensile misfit in one layer and compressive misfit in the other layer enhance both interaction energies. For example, $e^{I}_{aR,T}$ is more sensitive to a tensile misfit in the R layer whereas $e^{I}_{cR,T}$ is more sensitive to a compressive misfit in the R layer and tensile misfit in the T layer. In the case of PZT(40/60) bilayered system, the elastic interaction energies between *c* domain-R layer and *a* domain-R layer as a function of T and R layer misfits are shown in Fig. 3a and b, respectively. Here the increase of elastic interaction energies due to a tensile misfit in one layer and compressive misfit in the other layer is less pronounced than the PZT (20/80) system. This contrast between the two systems can be explained by the lower tetragonality of the PZT(40/60) in the T layer which results in lower self-strain. A reduced self-strain yields lower elastic interaction energies which can be justified by their definitions in Eqs. 25 and 26.

Figure 4a and b shows the total elastic energy of the PZT (20/80) system at equilibrium state versus misfits in the R and T layers, respectively. It is seen that the minimum equilibrium total energy is achieved when the misfit

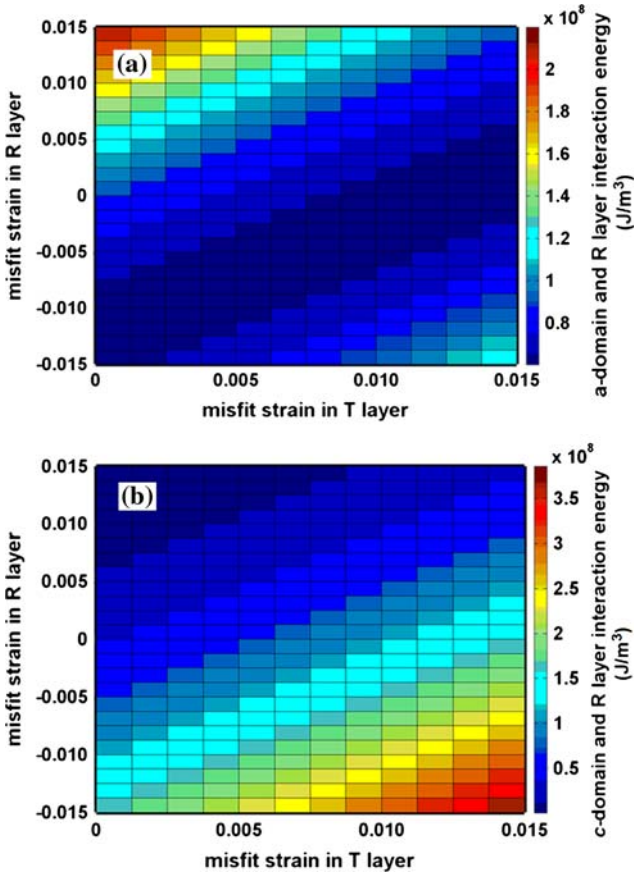

Fig. 2 **a** Interaction energies between *a*-domain and R layer versus misfit strains in the T and R layers in PZT20/80 system. **b** Interaction energies between *c*-domain and R layer versus misfit strains in the T and R layers in PZT20/80 system

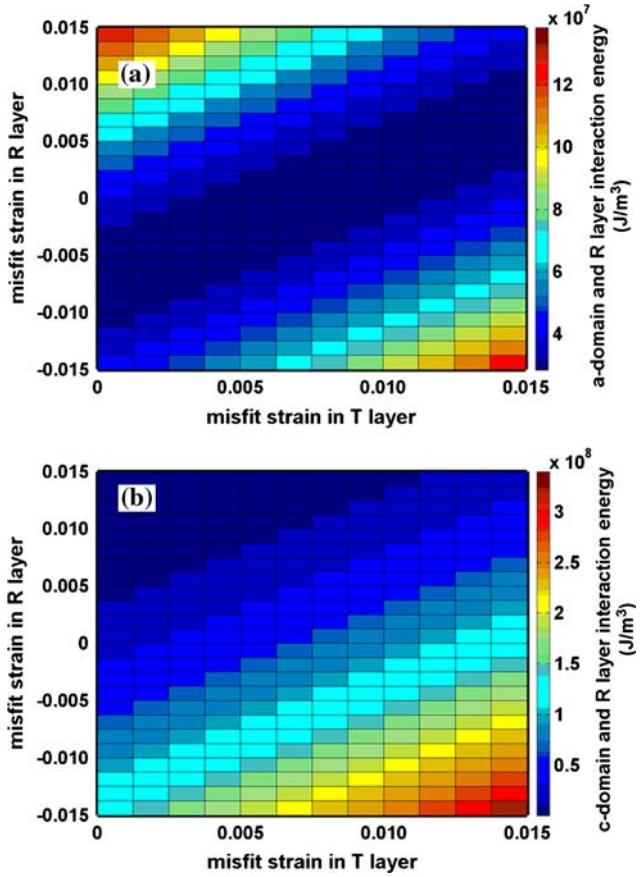

Fig. 3 **a** Interaction energies between *a*-domain and R layer versus misfit strains in the T and R layers in PZT40/60 system. **b** Interaction energies between *c*-domain and R layer versus misfit strains in the T and R layers in PZT40/60 system

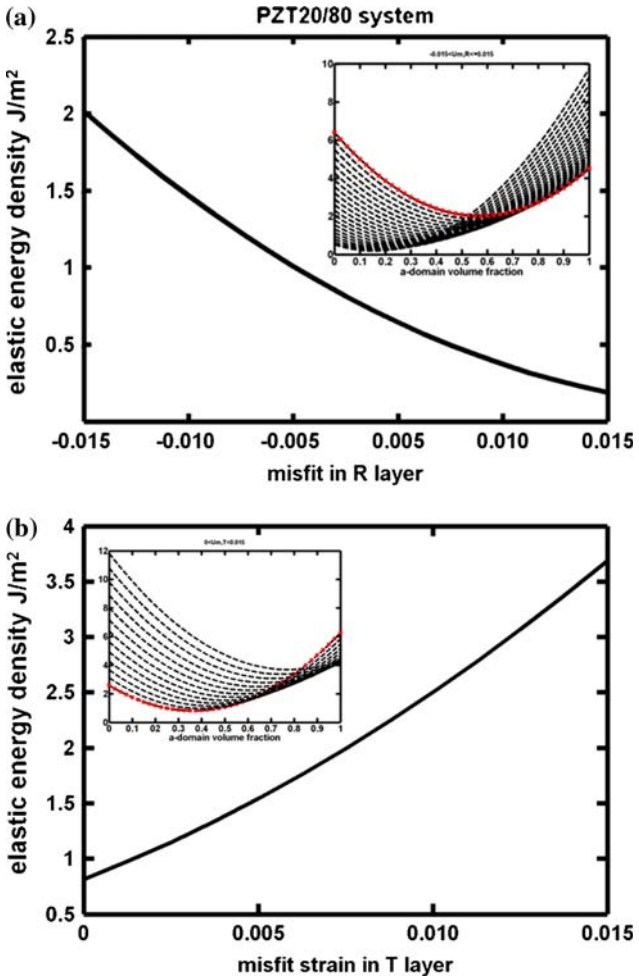

Fig. 4 **a** Total energy versus misfit in the R layer for PZT20/80 system. Inset: Total energies versus *a*-fraction for different misfit strains in the R layer. **b** Total energy versus misfit in the T layer for PZT20/80 system. Inset: Total energies versus *a*-fraction for different misfit strains in the T layer. The marked curves represent energies when misfit strain is −0.015

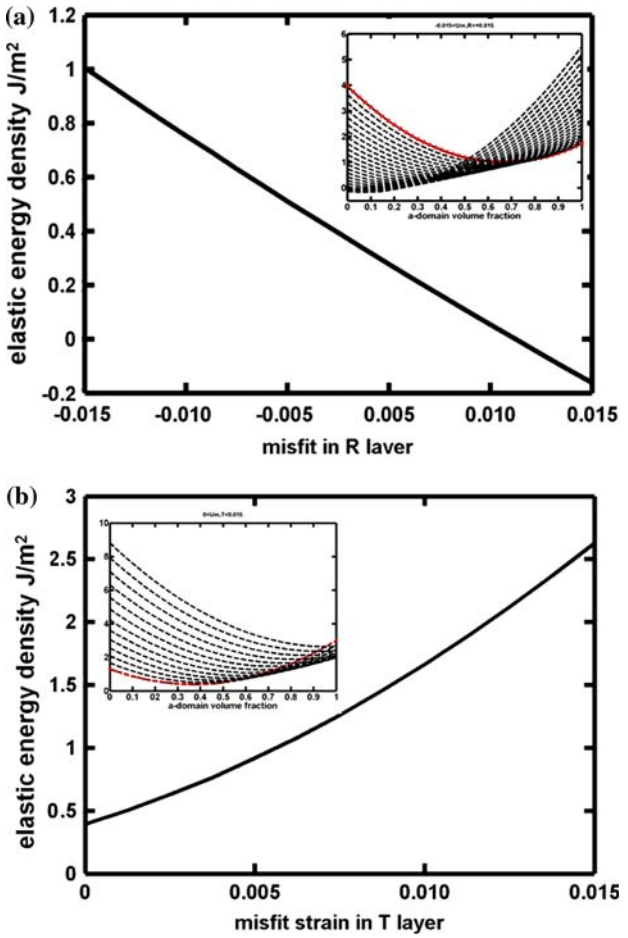

Fig. 5 **a** Total energy versus misfit in the R layer for PZT40/60 system. Inset: Total energies versus *a*-fraction for different misfit strains in the R layer. **b** Total energy versus misfit in the T layer for PZT40/60 system. Inset: Total energies versus *a*-fraction for different misfit strains in the T layer. The marked curves represent energies when misfit strain is −0.015

in the R layer is tensile and the misfit in the T layer is approaches compressive. The inset to Fig. 4a depicts the total elastic energy of the bilayer versus the equilibrium ferroelastic domain fraction. The misfit in the T layer is assumed relaxed due to the appearance of misfit dislocations and the misfit in the R layer is varied from −0.015 to +0.015. These diagrams show that the change of misfit in R layer from tensile to compressive increases the minimum total elastic energy. Moreover, the equilibrium ferroelastic domain fraction is also increased as the misfit in R layer goes from tensile to compressive. The inset to Fig. 4b depicts the total elastic energy of the bilayer versus the equilibrium ferroelastic domain fraction. Here the misfit in the R layer is assumed relaxed and the misfit in the T layer is varied from 0 to +0.015. It is seen that the change of misfit in T layer from tensile toward compressive decreases the minimum total elastic energy along with the equilibrium ferroelastic domain fraction. Figure 5a and b illustrates the total elastic energy of a PZT (40/60) system in terms of misfit strains in the R and T layers, respectively. The results are similar to those of PZT (20/80) system, albeit the lower tetragonalitiy of the PZT (40/60) system (as expected) results in lower equilibrium total elastic energy.

The properties discussed above can be summarized in Fig. 6 where the *a*-domain volume fraction is plotted as a function of the two misfit strains. Here a tensile misfit in T layer and a compressive misfit in R layer increase the *a*-domain fraction. Conversely, tensile misfit in R layer and less tensile misfit in T layer decrease the *a*-domain fraction. This opposite trend in the variation of ferroelastic domain fraction versus the two misfits in the bilayered structure can be attributed to the different self-strains induced in the

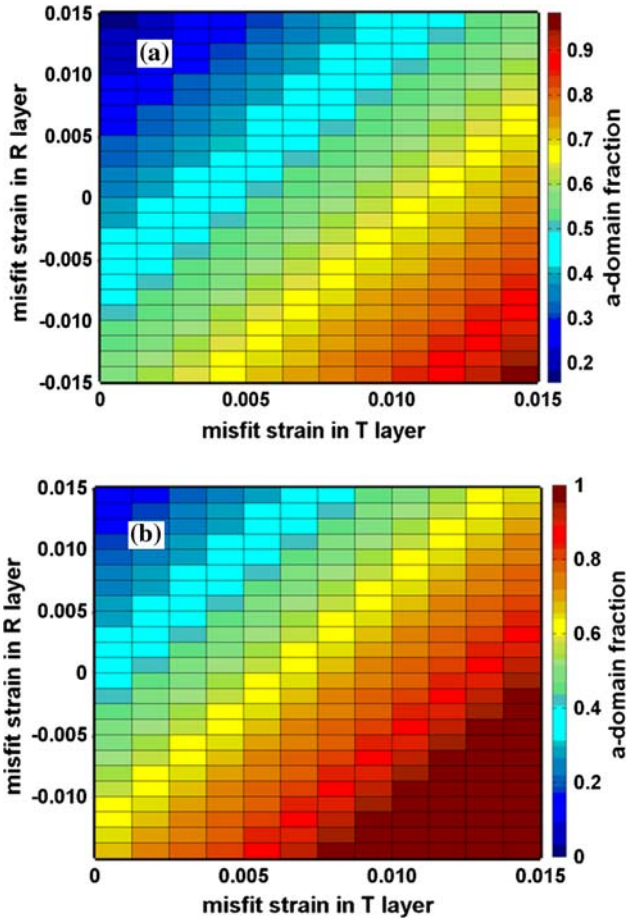

Fig. 6 **a** Equilibrium *a*-domain fraction versus misfit strains in T and R layers in PZT20/80 system. **b** Equilibrium *a*-domain fraction versus misfit strains in T and R layers in PZT40/60 system

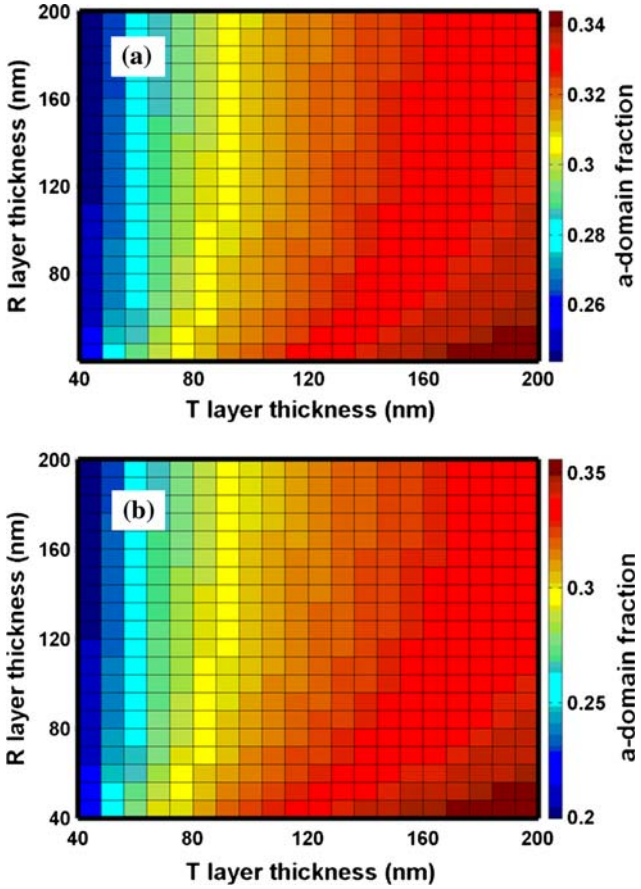

Fig. 7 **a** *a*-domain fraction versus thicknesses of T and R layers in PZT20/80 system. **b** *a*-domain fraction versus thicknesses of T and R layers in PZT40/60 system

ferroelastic domains of the T layer. More specifically, tensile self-strain is induced in *c*-domains and compressive self-strain is induced in *a*-domains, respectively. If the misfit strain in the T layer is assumed to be relaxed, then the *a*-fraction will vary from 0.2 to 0.6 as the misfit strain in the R layer changes from almost +0.015 (tensile) to −0.015 (compressive). Critically one finds that the *a*-domain fraction as a function of misfits forms a planar surface due to the fact that elastic energy is a quadratic function of strains. Similar to the previous results, the effect of the composition on the ferroelastic domains in the bilayer can be compared in Fig. 6a and b. It can be seen that PZT (20/80) system accommodates wider range of misfits in R and T layers before establishing single domain structure (fully *a* or *c*-domain) in the T layer.

This analysis can be farther extended to investigate the effect of film thickness in the multilayer structure by inspecting the formation of dislocations as the film thicknesses increase. Figure 7a and b illustrates the *a*-domain fraction as a function of T and R layer thicknesses in PZT(20/80) and PZT(40/60) systems grown on a model oxide cubic substrate ($SrTiO_3$), respectively. The curved surfaces of Fig. 7 depict the nonlinear effects of dislocations and the critical thickness of domain formation due to the contributions of domain walls to the total energy of the structure. It follows that when the film thickness is well above the critical thickness for dislocation formation; its variation has little effect on the volume fraction of ferroelastic structures in the tetragonal PZT. In other words, if the T layer thickness is increased 5 times from 40 to 200 nm, the *a*-fraction will be doubled from nearly 16% to 35%. This effect is even weaker in the R layer, i.e., the *a*-fraction will decrease from 26% to 16% if the R layer thickness is increased from 40 to 200 nm. However, a larger T layer thickness results in a larger relaxation of the misfit strain by dislocation formation which results in an increase in the *a*-domain fraction in the T layer.

Figure 8a and b is three-dimensional illustrations of dependence of ferroelastic domain fraction on field and misfit in the R layer in the PZT(20/80) and PZT(40/60) systems, respectively. They show that by switching the

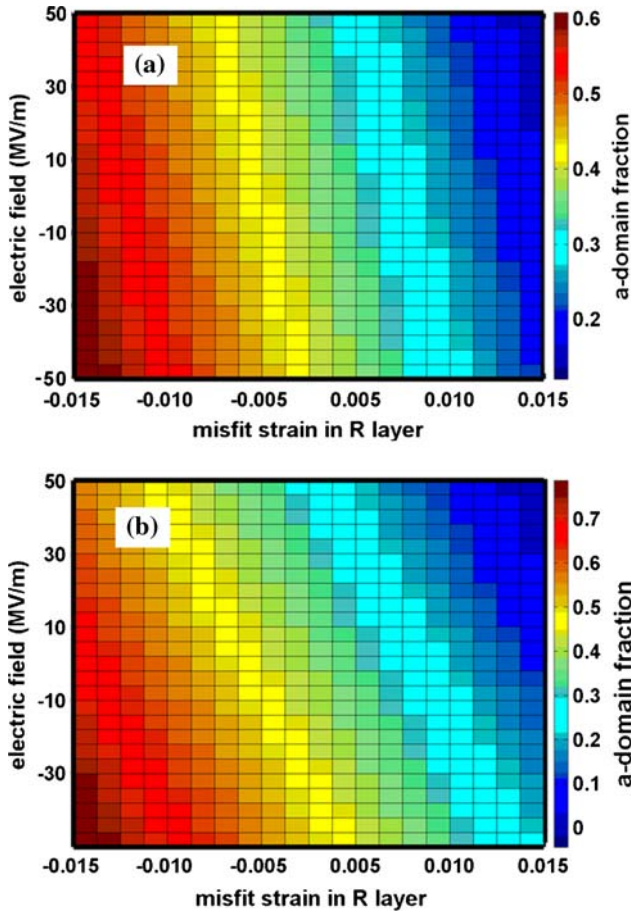

Fig. 8 **a** *a*-domain fraction versus electric field and misfit strain in R layer in PZT20/80 system. **b** *a*-domain fraction versus electric field and misfit strain in R layer in PZT40/60 system

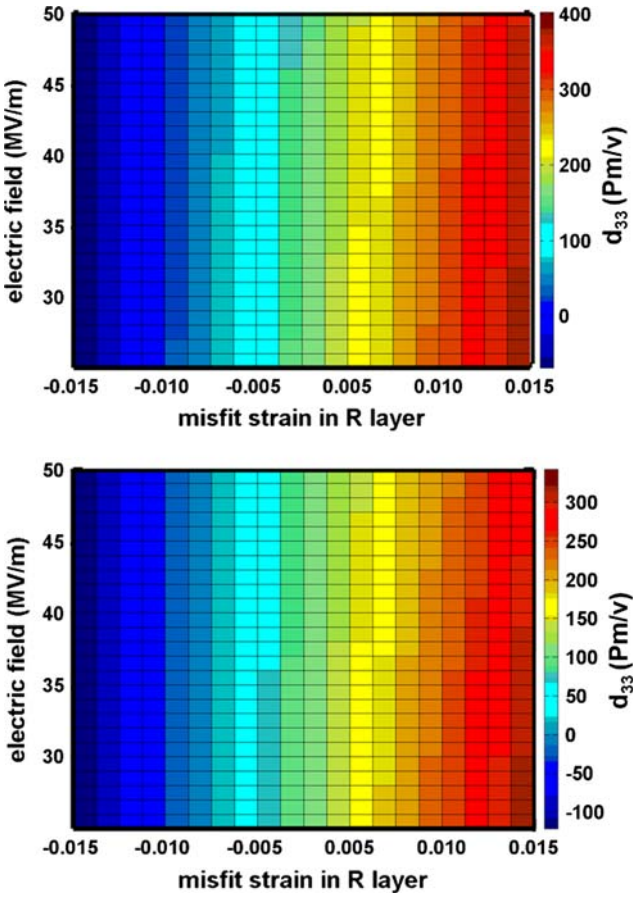

Fig. 9 **a** Effective d_{33} versus electric field and misfit strain in R layer in PZT20/80 system. **b** Effective d_{33} versus electric field and misfit strain in R layer in PZT40/60 system

polarity of the field the abundance of the ferroelastic domain fraction is increased (negative E) or decreased (positive E). The ferroelastic domain fraction varies linearly with respect to electric field because it is a linear function of strain and the piezoelectric effect is itself linear variation of strain in terms of the external electric field. It is shown that the misfit strain has a much stronger effect on ferroelastic domain abundance that the external electric field. In fact in PZT(20/80) system, the variation of electric field from −50 to +50 MV/m barely changes *a*-fraction by 10% whereas spanning misfit strain from +0.015 tensile to −0.015 compressive yields an almost sixfold increase of *a*-fraction from 10% to 60%. In the presence of external electric field, composition effect can be found by comparing Fig. 8a and b. Assuming a similar domain of misfit strain in the R layer, the PZT(40/60) system tunes *a*-domain fraction on a wider range than does the PZT(20/80) system.

The variation of effective out-of-plane piezoelectric constant d_{33} of the bilayer system can be seen in Fig. 9 in terms of changes in the misfit strain in the R layer and the external electric field. It is found that the effect of misfit strain is much stronger than the applied electric field on the effective piezoelectric coefficient. Moreover, at zero electric field and almost relaxed misfit between the film and the substrate, the d_{33} of the PZT(20/80) bilayer system is shown to be more than 150 pm/V namely, more than two or three times higher than previously reported monodomain value [32]. When the misfit tensile strain and the applied positive electric field are increased, the d_{33} of the bilayer system will increase to almost six times the bulk value. A comparison of Fig. 9a and b shows that as the content of Zirconium increases in the T layer, the d_{33} becomes less sensitive to both the applied field and the misfit strain.

Conclusions

Elastic interaction energies between the layers of a ferroelectric bilayer have been defined and analyzed in terms of the misfit strain induced into the layers and the structure composition. It was shown that these interaction energies

may lead to a substantial increase in the ferroelastic domain population of the tetragonal layer. Moreover, ferroelastic domain fraction and piezoelectric constant of the bilayered structure were numerically investigated in the presence of an external electric field. It was shown that piezoelectric constant values several times as high as the bulk value can be achieved.

Acknowledgements We would like acknowledge financial support from ARC DP0666231 and UNSW Faculty Research Grant.

References

1. Pontes FM, Longo E, Leite ER, Varela JA (2004) Appl Phys Lett 84:5470
2. Lee HN, Christen HM, Chisholm MF, Rouleau CM, Lowndes DH (2005) Nature 433:395
3. Cooper VR, Johnston K, Rabe KM (2007) Phys Rev B 76:020103
4. Vrejoiu I, Zhu Y, Rhun GL, Schubert MA, Hesse D, Alexe M (2007) Appl Phys Lett 90:072909
5. Wang C, Fang QF, Zhu ZG, Jiang AQ, Wang SY, Cheng BL, Chen ZH (2003) Appl Phys Lett 82:2880
6. Roytburd AL, Alpay SP, Nagarajan V, Ganpule CS, Aggarwal S, Williams ED, Ramesh R (2000) Phys Rev Lett 85:190
7. Zhou ZH, Xue JM, Li WZ, Wang J, Zhu H, Miao JM (2004) J Appl Phys 96:5706
8. Dawber M, Stucki N, Lichtensteiger C, Gariglio S, Ghosez P, Triscone JM (2007) Adv Mater 19:4153
9. Bungaro C, Rabe KM (2004) Phys Rev B 69:184101
10. Tian W, Jiang JC, Pan XQ, Haeni JH, Li YL, Chen LQ, Schlom DG, Neaton JB, Rabe KM, Jia QX (2006) Appl Phys Lett 89:092905
11. Roytburd AL, Zhong S, Alpay SP (2005) Appl Phys Lett 87: 092902
12. Roytburd AL (1998) J Appl Phys 83:228
13. Speck JS, Seifert A, Pompe W, Ramesh R (1994) J Appl Phys 76:477
14. Li JY, Liu D (2004) J Mech Phys Solids 52:1719
15. Davi F, Mariano PM (2001) J Mech Phys Solids 49:1701
16. Choudhury S, Li YL, Krill CE, Chen LQ (2005) Acta Mater 53:5313
17. Su Y, Landis CM (2007) J Mech Phys Solids 55:280
18. Burcsu E, Ravichandran G, Bhattacharya K (2004) J Mech Phys Solids 52:823
19. Freund LB, Nix WD (1996) Appl Phys Lett 69:173
20. Mahjoub R, Anbusathaiah V, Alpay SP, Nagarajan V (2008) J Appl Phys 104:124103
21. Roytburd AL (1998) J Appl Phys 83:239
22. Matthews JW, Blakeslee AE (1974) J Cryst Growth 27:118
23. Ouyang J, Roytburd AL (2006) Acta Mater 54:5565
24. Suhir E (1988) J Appl Mech Trans ASME 55:143
25. Speck JS, Pompe W (1994) J Appl Phys 76:466
26. Roitburd AL (1976) Phys Status Solidi A 37:329
27. Alpay SP, Roytburd AL (1998) J Appl Phys 83:4714
28. Chen L, Nagarajan V, Ramesh R, Roytburd AL (2003) J Appl Phys 94:5147
29. Haun MJ, Furman E, Jang SJ, McKinstry HA, Cross LE (1987) J Appl Phys 62:3331
30. Pertsev NA, Zembil'gotov AG, Wazer R (1998) Phys Solid State 40:2002
31. Nagarajan V, Jenkins IG, Alpay SP, Li H, Aggarwal S, Salamanca-Riba L, Roytburd AL, Ramesh R (1999) J Appl Phys 86: 595
32. Nagarajan V, Stanishevsky A, Chen L, Zhao T, Liu BT, Melngailis J, Roytburd AL, Ramesh R, Finder J, Yu Z, Droopad R, Eisenbeiser K (2002) Appl Phys Lett 81:4215